Synthesis of Highly Fluorinated Monodisperse Colloids for Low Refractive Index Crystalline Colloidal Arrays

Guisheng Pan, Albert S. Tse,[†] R. Kesavamoorthy,[‡] and Sanford A. Asher*

Contribution from the Department of Chemistry, University of Pittsburgh, Pittsburgh, Pennsylvania 15260

Received February 12, 1998

Abstract: Highly charged fluorinated monodisperse spherical particles of diameters between 50 and 250 nm were synthesized from 1H,1H-heptafluorobutyl methacrylate by emulsion polymerization. These particles have a low refractive index of 1.386. High particle surface charge densities were obtained by minimizing the polymer molecular weight. These colloids formed well-ordered crystalline colloidal arrays (CCAs), after dialysis and ion exchange, which Bragg diffract light at wavelengths from the near-IR down to 270 nm in the UV. The diffraction bandwidths in water are very narrow (<10 nm) due to the closeness of refractive index of the colloidal particles to that of water. These CCAs are excellent materials for narrow band notch optical filters. In addition, these fluorinated CCAs can be easily refractive index matched to a predominately aqueous medium. We have covalently attached dyes to the colloidal particles to prepare absorbing CCAs. We photopolymerized these dyed CCAs within a polyacrylamide matrix to form polymerized crystalline colloidal array (PCCA). These semisolid PCCAs can withstand vibrations, ionic impurity addition, and thermal shocks while maintaining the CCA ordering. The medium within the PCCA can easily be exchanged to exactly refractive index match the CCA. These refractive index matched dyed PCCAs may have applications in optical limiting, computing, and nanosecond fast optical switching devices as discussed in the accompanying paper.

Introduction

Charged monodisperse colloidal particles suspended in deionized aqueous solution can self-assemble into three-dimensional periodic structures called crystalline colloidal arrays (CCAs).[1−6] The driving force behind this spontaneous ordering is the strong Coulombic repulsive interactions between the charged particles.[3,5] To minimize the system energy, the colloidal particles self-assemble into either body-centered cubic (bcc) or face-centered cubic (fcc) crystal structures. The CCA usually orients with the highest particle density crystal planes (bcc (110) or fcc (111)) parallel to the container walls.[2,6−9]

CCAs are mesoscopic analogues of atomic crystals.[3,5,10] The particle diameters are on the order of hundred nanometers, and the interparticle spacings can be several times the particle diameter. Thus, instead of diffracting X-rays as atomic crystals, CCAs Bragg diffract electromagnetic radiation in the ultraviolet, visible, and near-infrared spectral regions.[4,6] The CCAs differ from atomic crystals in that their volume fractions, particle diameters, and the interparticle interactions can be varied over a wide range.[7,8] In addition, the modulation in the optical dielectric constants in the CCAs between the particles and the surrounding medium is much larger than that which occurs in atomic crystals. Therefore, the diffraction efficiency of CCAs is remarkably high. For example, the transmission of a few hundred micrometer thick polystyrene CCAs can be as small as 10^{-8}.[7,11] These unique properties of CCAs have been utilized to make devices such as narrow band optical rejection filters,[4,11−17] novel nonlinear nanosecond optical limiting and switching devices,[18−21] and chemical sensing devices.[22]

A major drawback of liquid CCAs is that weak shear, gravitational, electrical, and thermal forces can disturb the crystalline ordering.[2,3,23,24] More robust CCA materials would

* To whom correspondence should be addressed. Phone: 412-624-8570. Fax: 412-624-0588. E-mail: Asher+@pitt.edu.

[†]Reichhold Chemicals, Research Triangle Park, NC 27709.

[‡] Permanent address: Materials Science Division, Indira Gandhi Center for Atomic Research, Kalpakkam 603 102, Tamil Nadu, India.

(1) Krieger, I. M.; O′Neill, F. M. *J. Am. Chem. Soc.* **1968**, *90*, 3114−3120.
(2) Clark, N. A.; Hurd, A. J.; Ackerson, B. J. *Nature* **1979**, *281*, 57−60.
(3) Pieranski, P. *Contemp. Phys.* **1983**, *24*, 25−73.
(4) Flaugh, P. L.; O′Donnell, S. E.; Asher, S. A. *Appl. Spectrosc.* **1984**, *38*, 847−850.
(5) Sood, A. K. *Solid State Physics*; Ehrenreich, H., Turnbull, D., Eds.; Academic Press: New York, 1991; Vol. 45, pp 1−73.
(6) Carlson, R. J.; Asher, S. A. *Appl. Spectrosc.* **1984**, *38*, 297−304.
(7) Rundquist, P. A.; Photinos, P.; Jagannathan, S.; Asher, S. A. *J. Chem. Phys.* **1989**, *91*, 4932−4941.
(8) Monovoukas Y.; Gast, A. P. *J. Colloid Interface Sci.* **1989**, *128*, 533−548.
(9) Kesavamoorthy, R.; Tandon, S.; Xu, S. Jagannathan, S.; Asher, S. A. *J. Colloid Interface Sci.* **1992**, *153*, 188−198.
(10) Sanders, J. V. *Nature* **1964**, *204*, 1151−1153.
(11) Asher, S. A.; Flaugh, P. L.; Washinger, G. *Spectroscopy* **1986**, *1*, 26−31.
(12) Asher, S. A. U.S. Patents 1986, Nos. 4 627 689 and 4 632 517.
(13) Spry, R. J.; Kosan, D. J. *Appl. Spectrosc.* **1986**, *40*, 782−784.
(14) Jethmalani, J. M.; Ford, W. T. *Chem. Mater.* **1996**, *8*, 2138−2146.
(15) Jethmalani, J. M.; Sunkara, H. B.; Ford, W. T. *Langmuir* **1997**, *13*, 2633−2639.
(16) Jethmalani, J. M.; Ford, W. T.; Beaucage, G. *Langmuir* **1997**, *13*, 3338−3344.
(17) Weissman, J. M.; Sunkara, H. B.; Tse, A. S.; Asher, S. A. *Science* **1996**, *274*, 959−960.
(18) Runquist, P. A.; Jagannathan, S.; Kesavamoorthy, R.; Brnardic, C.; Xu, S.; Asher, S. A. *J. Chem. Phys.* **1991**, *94*, 711−717.
(19) Kesavamoorthy, R.; Jagannathan, S.; Rundquist, P. A.; Asher, S. A. *J. Chem. Phys.* **1991**, *94*, 5172−5179.
(20) Kesavamoorthy, R.; Super, M. S.; Asher, S. A. *J. Appl. Phys.* **1992**, *71*, 1116−1123.
(21) Pan, G.; Kesavamoorthy, R.; Asher, S. *Phy. Rev. Lett.* **1997**, *78*, 3860−3863.
(22) Holtz, J. H.; Asher, S. A. *Nature* **1997**, *389*, 829−832.
(23) Crandall, R. S.; Williams, R. *Science* **1977**, *198*, 293−295.
(24) Tomita, M.; van de Ven, T. G. M. *J. Phys. Chem.* **1985**, 89, 1291−1296.

S0002-7863(98)00482-X CCC: $15.00
Published on Web 06/18/1998

be more useful for optical devices. Recently, synthetic methods have been developed to photopolymerize CCAs in polyacrylamide hydrogels[17,25−27] and polymethyl methacrylate[14−16] matrixes, which permanently lock in the ordering. These solid polymerized CCAs (PCCAs) can withstand vibrations, ionic species addition, and thermal shocks, while maintaining the CCA ordering. Moreover, the medium refractive index of the CCA solidified in the polyacrylamide hydrogel networks can be adjusted by exchanging the aqueous solvent inside the matrix. This property can be utilized to control the refractive index mismatch between the particles and their surrounding medium.

Here we describe the synthesis of a new type of colloidal particles which has an extraordinarily low refractive index, which also contains absorbing dyes. We also describe the polymerization of a CCA of these particles into a hydrogel matrix. In an accompanying paper we describe the use of these materials for nanosecond response nonlinear optical switching. The idea is to refractive index match the dyed particles to the aqueous medium, such that the real part of the refractive index is homogeneous throughout, but where the CCA periodicity exists in the imaginary part of the refractive index. This array will be highly optically nonlinear to incident pulsed lasers at wavelengths absorbed by the dye. The colloidal particles will heat up, and the real part of the refractive index of the particles will diverge from that of the medium; the array will "pop up" to Bragg diffract light. This system will act as an optical limiter or optical switch.[20,21,28,29]

Previously reported colloidal particles made from common polymers such as PMMA are difficult to refractive index match due to their relatively high refractive indexes ($n_D = 1.490$ for PMMA). To refractive index match these particles to the suspension medium, we previously attempted to utilize high refractive index nonaqueous solvents such as methyl phenyl sulfoxide ($n_D = 1.577$), which is water-miscible, in the CCA or PCCA.[30] However, the ordering of the CCA is perturbed by large amounts of these types of materials. Thus, it was necessary to fabricate highly charged monodisperse particles of low refractive index. Highly fluorinated polymers are known to have extremely low refractive indexes. Poly(tetrafluoroethylene) (PTFE), for example, has a refractive index of 1.35. Unfortunately PTFE is crystalline and optically heterogeneous, and thus impossible to refractive index match.[31,32]

Experimental Section

Reagents. 1H,1H−Heptafluorobutyl methacrylate (FBMA) and ethylene glycol dimethacrylate (EGDMA) were obtained from Lancaster Synthesis Inc. and were used after removing inhibitors by using an alumina column. The Aerosol MA 80-I surfactant contains sodium di(1,3-dimethylbutyl)sulfosuccinate, 2-propanol, methyl isobutyl carbinol, and water and was obtained from American Cyanamid. Sodium persulfate, dimethyl sulfoxide (DMSO), methyl phenyl sulfoxide (MPSO), and 2,2-diethoxyacetophenone were obtained from Aldrich. Acrylamide and *N*,*N*′-methylenebisacrylamide were obtained from Fluka. These chemicals were used as received. Acylated Oil Blue N dye was synthesized according to the procedure of ref 30. Mixed bed ion-exchange resin (AG 501-X8, 20−50 mesh) was purchased from Bio-Rad Lab. Deionized water was obtained from a Nanopure System (Barnstead/Thermolyne Co.).

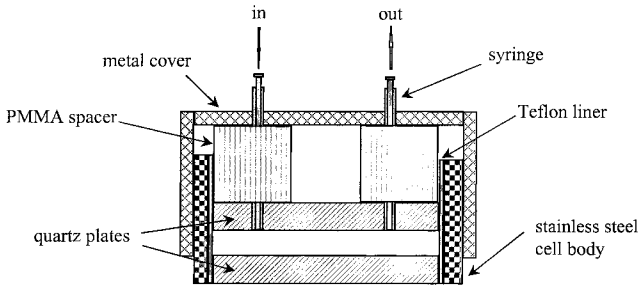

Figure 1. Variable path length sample cell. The upper quartz plate was glued to a transparent PMMA spacer which was attached to the metal cover. CCA solutions were injected into the cell through the syringes. The upper quartz plate, along with the PMMA spacer and the metal cover, was rotated to adjust the path length between 0 and 5 mm.

Colloid Synthesis. Poly(1H,1H-heptafluorobutyl methacrylate) (PFBMA) particles were synthesized by free-radical emulsion polymerization. The polymerization was carried out in a 50-mL three-neck round-bottom flask equipped with a reflux condenser, nitrogen inlet, thermometer, and a magnetic stirrer. The flask was immersed in a water bath thermostated at the 50 °C reaction temperature. The reactor was charged with the deionized water, Aerosol MA 80-I, FBMA, EGDMA, and acylated Oil Blue N (if used). The contents were stirred and flushed with nitrogen for about 30 min. The initiator ($Na_2S_2O_8$), dissolved in a small amount of water, was then injected into the reactor to start the reaction. The polymerizations were carried out under a nitrogen atmosphere for 3 h.

Colloid Purification. The colloids were dialyzed against deionized water with the use of dialysis membranes (Spectra/Por, MWCO = 50 000) by changing the water daily until the specific conductivity was constant (∼1 μS/cm). Further purification was achieved by shaking the latexes with ion-exchange resin in a shaker for at least one week. The suspensions then showed iridescent color, indicating the formation of a CCA.

PCCA Synthesis. To polymerize the CCA in a hydrogel matrix, we mixed 0.0714 g of acrylamide (monomer), 0.0055 g of *N*,*N*′-methylenebisacrylamide (cross-linker), and 0.0012 g of 2,2-diethoxyacetophenone (photoinitiator) with 0.9243 g of CCA. After the mixture was shaken with ion-exchange resin for 8 h, the CCA mixture was injected into the cell. The CCA was then polymerized for 8 h under a UV Hg light irradiation lamp (Blak-Ray model B-100A, UVP Inc.).

Colloid and CCA Characterization. The particle diameter and distribution of the colloids were determined by quasi-elastic light scattering (QELS)[33] using a Malvern Zetasizer 4. The particles were also examined by transmission electron microscopy (TEM). The surface charge densities of the latexes were determined by conductometric titration. Standard (0.01 N) NaOH solution was used to titrate 10 mL of purified samples with a solid's content of ∼10%. The specific conductivity was measured by a conductance meter (YSI model 35). The solid's content of the latex was determined by drying a weighed amount of colloidal suspension at 105 °C. The volume fraction of particles in the suspension was then calculated from the solid's content and the specific density of the colloidal particles. The particle specific density was determined to be 1.580 at room temperature by using a 10-mL pycnometer. The total volume of a colloid solution is the sum of volume for both water and particles. If one knows the total weight, total volume, and the solid's content of the colloid, the particle density can be calculated. The refractive index was measured by an Abbe

(25) Haacke, G.; Panzer, H. P.; Magliocco, L. G.; Asher, S. A. U.S. Patent 1993, No. 5 266 238.
(26) Kamenetsky, E. A.; Magliocco, L. G.; Panzer, H. P. *Science* **1994**, *263*, 207.
(27) Asher, S. A.; Holtz, J.; Liu, L.; Wu, Z. *J. Am. Chem. Soc.* **1994**, *116*, 4997−4998.
(28) Asher, S. A.; Kesavamoorthy, R.; Jagannathan, S.; Rundquist, P. *SPIE, Nonlinear Optics III* **1992,** *1626*, 238−242.
(29) Asher, S. A.; Chang, S.-Y.; Jagannathan, S.; Kesavamoorthy, R.; Pan, G. U.S. Patent 1995, No. 5 452 123.
(30) Tse, A. S.; Wu, Z.; Asher, S. A. *Macromolecules* **1995**, *28*, 6533−6538.
(31) Piazza, R.; Stavans, J.; Bellini, T.; Lenti, D.; Vica, M.; Degiorgio, V. *Prog. Colloid Polym. Sci.* **1990,** *81*, 89−94.
(32) Degiorgio, V. *The Structures, Dynamics and Equilibrium Properties of Colloidal Systems*; Bloor, D. M., Wyn-Jones, E., Eds.; Kluwer Academic Publishers: Netherlands, **1990**; pp 583−596.
(33) Berne, B. J.; Pecora, R. *Dynamic Light Scattering*; John Wiley & Sons: New York, 1976; pp 10−52.

Table 1. Initial-Charge Polymerization Recipes

	recipe 1	recipe 2
reagents (g)		
FBMA	4.0	10.0
EGDMA	0.15	0.15
Aerosol MA 80-I	0.10	0.10
Acylated Oil Blue N	0	0.032
sodium persulfate	0.20	0.16
water	20	20
reaction temperature (°C)	50	55
reaction time (h)	3.0	3.0
particle diameter (nm)	104	138

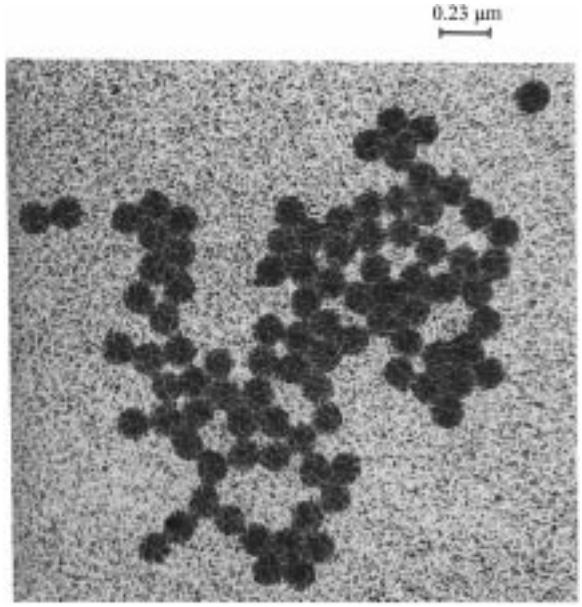

Figure 2. TEM picture of gold-coated PFBMA particles. The average particle diameter is 137 nm and the standard deviation is 3.4%.

refractometer at 589 nm. The specific heat was measured by differential scanning calorimetry (DSC). Turbidity was measured by Perkin-Elmer model Lambda 9 Spectrometer.

Transmission spectra of the CCA were obtained by using a Perkin-Elmer model Lambda 9 Absorption Spectrometer. The sample cell used was a specially designed variable path length quartz cell consisting of quartz plates and a Teflon liner (Figure 1). The CCA liquid was injected into the cell by using a syringe. The upper quartz plate was rotated to adjust the path length between the quartz plates. The sample plane was always horizontal during the development of CCA. In Figure 1, the incident light passes through the optical cell from the bottom to the top.

Results and Discussion

Colloid Synthesis and Characterization. We utilized an initial-charge emulsion polymerization technique.[34] Two recipes are given in Table 1 for the particles in the absence or presence of dye. The solid's content and the particle size leveled out after 1 h. The TEM photograph (Figure 2) shows that the particles are monodisperse spheres. The average diameter is 137 nm with a standard deviation of 3.4%.

Effect of Surfactant Concentration on Particle Diameter. We examined the dependence of the particle size on the surfactant concentration. A monotonic decrease in particle size occurs as the Aerosol MA 80-I surfactant concentration increases (Figure 3). The particle diameter can be controlled between 50 and 250 nm by adjusting the surfactant concentration. In these syntheses, we used 0.020 g of $Na_2S_2O_8$ instead of 0.20 g as listed in Table 1. Therefore the particle diameters in Figure 3 are different from those indicated in Table 1.

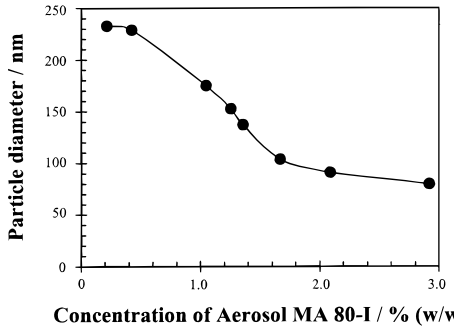

Figure 3. Dependence of particle diameter on surfactant concentration. Same amount of $Na_2S_2O_8$ initiator (0.020 g) was used in the syntheses.

Table 2. Dependence of Particle Surface Charge Density on $Na_2S_2O_8$ Concentration[a]

batch	$Na_2S_2O_8$ (mM)	diameter (nm)	charge density (μC/cm^2)
GP262	4.2	106	0.22
GP263	10.5	100	0.23
GP264	21.0	92	0.25
GP265	42.0	74	0.48
GP266	84.0	73	0.58

[a] The concentration of Aerosol MA 80-I was kept at 0.82% (w/w).

Table 3. Dependence of Particle Surface Charge Density on $Na_2S_2O_8$ and $C_{12}H_{25}SH$ Concentrations[a]

batch	$Na_2S_2O_8$ (mM)	$C_{12}H_{25}SH$ (mM)	diameter (nm)	charge density (μC/cm^2)
GP224	4.2	6.5	93	0.77
GP223	21.0	26.0	153	1.02
GP225	42.0	51.1	107	1.03

[a] Reaction temperature was 70 °C. The concentration of Aerosol MA 80-I was 0.73% (w/w).

Optimization of Particle Surface Charge Density. The effect of initiator on charge density was investigated by varying the concentration of sodium persulfate until coagulation occurs (above 90 mM). Table 2 shows that the surface charge density increases as the initiator concentration increases. It is well-known that the polymer molecular weight decreases as the initiator concentration increases.[35] Since particles consist of many entangled polymer chains attached to ionizable end groups (sulfate), shorter polymer chains will give higher charge densities. Equation 11 in the appendix shows that the charge density is inversely proportional to the polymer molecular weight.

As shown in Table 2, the particles have surface charge densities almost as high as 0.60 μC/cm^2, which indicates a molecular weight M_n of 3.2×10^5. Thus, the polymer molecular weight is still relatively high. We should be able to further increase the surface charge density by increasing the reaction temperature and using a chain transfer agent like mercaptan to further decrease the polymer molecular weight.[35] The charge density was increased up to 1.0 μC/cm^2 in the presence of $C_{12}H_{25}SH$ for a reaction temperature of 70 °C (Table 3).

The particle specific heat was measured between 25 and 140 °C by differential scanning calorimetry (DSC) as shown in Figure 4A. The glass transition occurs at 62 °C, close to the

(34) Chainey, M.; Wilkinson, M. C.; Hearn, J. *Ind. Eng. Chem. Prod. Res. Dev.* **1982,** *21*, 171−176.

(35) Bovey, F. A.; Kolthoff, I. M.; Medalia, A. I.; Meehan, E. J. *Emulsion Polymerization*; Interscience Publishers: New York, 1955; pp 95−139.

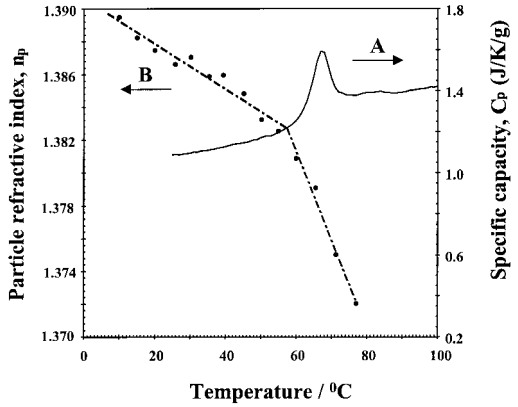

Figure 4. (A) Temperature dependence of heat capacity of PFBMA polymer determined by differential scanning calorimetry. The scanning rate was 10 °C/min. (B) Temperature dependence of PFBMA particle refractive index. The glass transition occurs at 58 °C. $dn_p/dT = -1.39 \times 10^{-4}$/°C (below 58 °C) and -5.40×10^{-4}/°C (above 58 °C).

reported T_g value (65 °C) for the bulk polymer.[36] An endothermic peak shown at about 67 °C close to T_g probably results from melting of the crystalline portion of this colloidal polymer.

We determined the refractive index of the colloidal particles by turbidity measurements. The turbidity (T) is

$$T = (1/b)\ln(I_0/I_t) \tag{1}$$

where b is the cell thickness, I_0 and I_t are the incident and transmitted light intensities, respectively. The turbidity is given by[31]

$$T = N\sigma \tag{2}$$

where N is the number concentration of particles and σ is the total scattering cross-section. In our case, where the particle diameter is ~100 nm and the refractive index ratio (m) between the particle (n_p) and the medium (n_m) is very close to 1, the $m-x$ domain falls in category 1 of van de Hulst.[37] Thus, the total scattering cross-section can be expressed as[37]

$$\sigma = A(m-1)^2 \tag{3}$$

where A is a function of the particle diameter and the scattered wavelength. By combining eqs 2 and 3, we have the specific turbidity (T/N):

$$T/N = B(n_p - n_m)^2 \tag{4}$$

where B is a constant for a given particle size and a scattered wavelength. When $n_m = n_p$, T/N goes to zero. Thus, the refractive index of the particles can be determined from this point.

A series of ethylene glycol/water solutions was prepared with refractive indices ranging from 1.33 to 1.41. A dialyzed latex sample (~0.1 g) with a solid's content of ~15% was added to 1.0 g of the ethylene glycol/water solutions. The suspension turbidities were then measured in a 1 cm thick quartz optical cell at 589 nm and at 25 °C. Before each turbidity measurement, the surface reflection was corrected by a blank sample made from the corresponding ethylene glycol/water solution. The refractive indexes of the blank solutions were measured at 589 nm and at 25 °C using an Abbe refractometer.

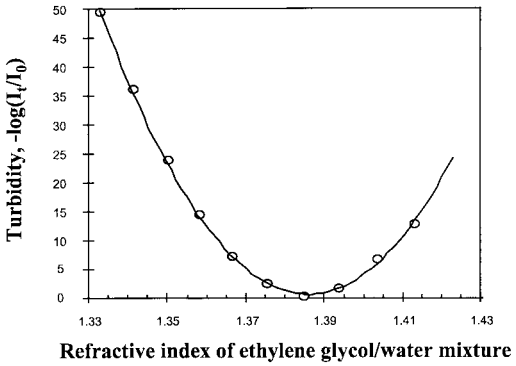

Figure 5. Dependence of the specific turbidity of a PFBMA colloidal suspension on the suspension medium refractive index (see text for details).

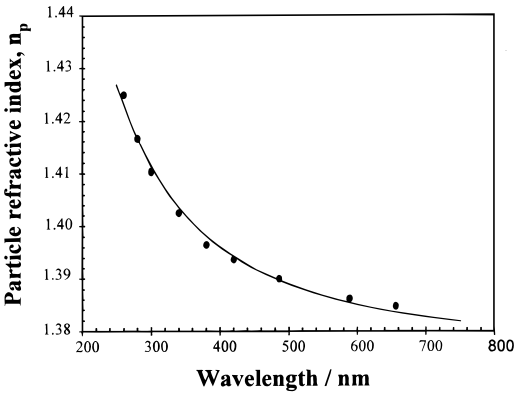

Figure 6. Refractive index dispersion curve of PFBMA colloidal particles at 25 °C.

Figure 5 shows the dependence curve of the specific turbidity (T/N) on n_m. This curve is parabolic as expected and fits to a quadratic equation: $T/N = an_m^2 + bn_m + c$. The refractive index of PFBMA colloidal particles was determined to be 1.3860 from the minimum point where $d(T/N)/dn_m = 0$. This is very close to the literature value reported for bulk PFBMA polymer (1.383).[36]

Similarly, we determined the refractive indexes of the PFBMA colloidal particles at the wavelengths other than 589 nm. Turbidities were measured in the range of 200 to 700 nm. The refractive indexes of water and ethylene glycol between 200 and 700 nm were obtained from the literature.[38-40] The refractive indexes (n_m) of the solvent was calculated from

$$n_m = n_w\Phi_w + n_{eg}(1-\Phi_w) \tag{5}$$

Here, n_w and n_{eg} are the refractive indexes of water and ethylene glycol, respectively. Φ_w is the volume fraction of water in the mixture. Figure 6 shows the dispersion curve of PFBMA colloidal particles between 250 and 700 nm. The data are well fit by

$$n_p = 1.3763 + 3159.7/\lambda^2 \tag{6}$$

where λ is the wavelength (nm).

We determined the temperature dependence of n_p at 589 nm (Figure 4B) by using a temperature controlled Abbe refractometer. The colloidal particles, suspended in water, were equilibrated at temperatures ranging from 10 to 80 °C for ~10

(36) Gaynor, J.; Schueneman, G.; Schuman, P.; Harmon, J. P. *J. App. Polym. Sci.* **1993**, *50*, 1645−1653.
(37) van de Hulst, H. C. *Light Scattering by Small Particles*; Dover Publications: New York, 1981; p 134.
(38) Duclaux, J.; Jeantet, P. *J. Phys.* **1924**, *5*, 92−94.
(39) Karvonen, A. *Ann. Acad. Sci. Fenn.* **1916**, *10A*, 1−22.
(40) Voellmy, H. *Z. Phys. Chem. Stoechiom. Verwandtschaftsl* **1927**, *127*, 306−357.

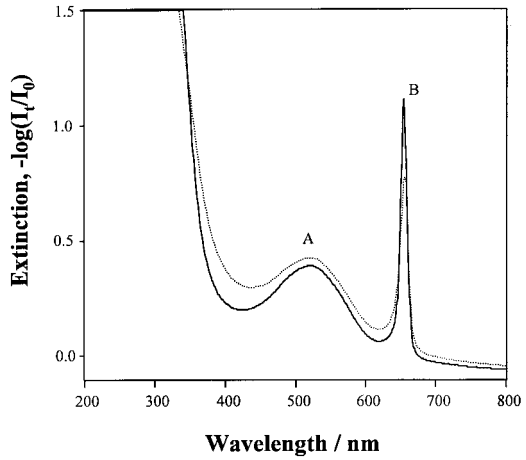

Figure 7. Transmission spectra of absorbing CCA before and after photopolymerization. Acylated Oil Blue N dye was covalently attached to the PFBMA particles. Peak A is the dye absorption band. Peak B results from the Bragg diffraction. The spectra before and after photopolymerization are shown in solid and dashed lines, respectively. The absorbing CCA was 0.80 mm thick. The particle diameter was 138 nm.

min, and the suspension refractive index, n, and water refractive index, n_w, were measured at 589 nm. The measured water refractive index at all temperatures agreed well with the literature.[41] The change in the slope at 58 °C presumably signals the glass transition. However, 58 °C is four degrees lower than the T_g value determined by DSC measurements. This may indicate a decreased T_g for the particles in water or that the DSC measured T_g was too high due to a time lag in the sample response.[42]

Absorbing Polymerized CCA. We covalently attached the polymerizable dye, acylated Oil Blue N, to the PFBMA particles during the emulsion polymerization. A typical recipe is given in Table 1. These dyed fluorinated colloids readily self-assemble into a CCA which we then photopolymerized within a polyacrylamide hydrogel. Figure 7 shows the −log transmission spectrum of an absorbing CCA before and after photopolymerization. Peak A results from the absorption of acylated Oil Blue N dye. Peak B indicates the Bragg diffraction wavelength maximum which remains unchanged after photopolymerization. The extinction, defined by $E = -\log(I_t/I_0)$, decreases somewhat, probably because the lattice ordering is slightly perturbed.

Effect of CCA Thickness. It is known that the CCA near the container walls are better ordered than those in the center region.[2,43−45] The degree of ordering should influence the diffraction intensity. We examined the CCA thickness dependence of the extinction (Figure 8). After the CCA was injected into the cell, transmission spectra were taken every 6 h until the extinction became constant. The typical annealing time was 1 day. As seen from the insert of Figure 8, the extinction first linearly increases as the CCA thickness increases (up to ∼0.5 mm) and then levels off when $E \approx 2.5$ because of spectrometer stray light. According to diffraction theory, the extinction

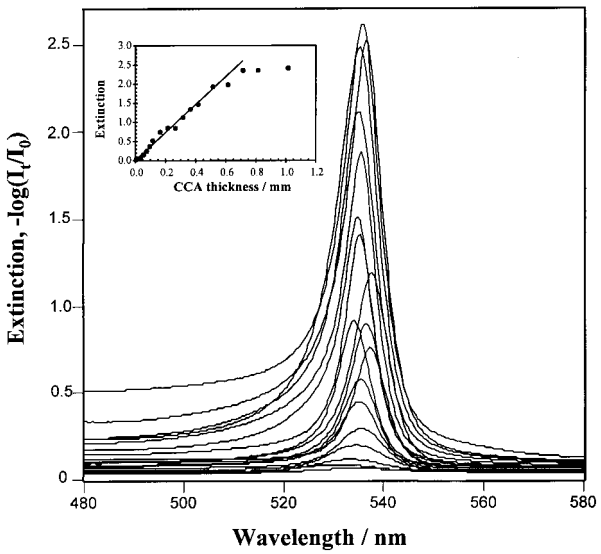

Figure 8. Transmission spectra of PFBMA CCA at thicknesses of 1.015, 0.815, 0.715, 0.615, 0.515, 0.415, 0.365, 0.315, 0.265, 0.215, 0.165, 0.115, 0.095, 0.075, 0.055, 0.035, 0.015, and 0.005 mm, respectively. The particle diameter was 130 nm. The particle volume fraction was 11.86%.

should be proportional to the crystal thickness.[46] Our data agrees with this prediction. However, if the ordering degree differed for the CCA near and away from the container walls, we would not expect the linear curve shown in Figure 8.

We examined the thickness dependence by polymerizing CCAs of varying thicknesses between 0.2 and 1 mm in a polyacrylamide hydrogel matrix. The polymerized CCA was cut out and its cross-section was examined in a microscope. Three distinct regions were observed for 1 mm thick solidified CCA. Two well-ordered regions (∼0.3 mm thick) occurred next to the container walls while the central region was less ordered. Less than 0.6 mm thick CCA did not show the less ordered central region. Thus, the lattice ordering was uniform throughout the CCA for thicknesses less than ∼0.6 mm. This is consistent with the linear relationship between the extinction and the CCA thickness in Figure 8.

The observed bandwidths of the PFBMA CCA are quite narrow (fwhm ≈ 8 nm, Figure 8). The theoretical bandwidth ($\Delta\lambda_0$) can be calculated from[13]

$$\Delta\lambda_0 = \frac{8}{9\pi^2}\kappa\left(\frac{\lambda_0}{2}\right)(m^2-1)\left(\frac{3}{m^2+2}\right)\frac{(\sin u - u\cos u)}{\sin^2\theta} \quad (7)$$

where κ, the polarization factor, is equal to unity for unpolarized normally incident light. λ_0 is the wavelength in air, m is the refractive index ratio between the particles and the medium, θ is the Bragg angle, and u is the scattering parameter:

$$u = \frac{2\pi n D_0}{\lambda_0}\sin\theta \quad (8)$$

where D_0 is the particle diameter, n is the refractive index of the suspension. Using $m = 1.386/1.333$, $\Phi_w = 1-0.1186 = 0.8814$, $n = 1.333\Phi_w + 1.386(1-\Phi_w) = 1.339$, $\lambda_0 = 535$ nm, $D_0 = 130$ nm, $\theta = 90°$, $u = 2.045$ (eq 8), we calculate $\Delta\lambda_0 = 1.1$ nm. Our measured bandwidths are larger than those calculated, presumably because the CCA contains microcrys-

(41) *CRC Handbook of Chemistry and Physics*, 50th ed.; CRC Press: Cleveland, 1969; p E-232.
(42) Sperling, L. H. *Introduction to Physical Polymer Science*; John Wiley & Sons: New York, 1992; p 323.
(43) Kesavamoorthy, R.; Rajalakshmi, M.; Babu Rao, C. *J. Phys.: Condens. Matter* **1989**, *1*, 7149−7161.
(44) Kesavamoorthy, R.; Babu Rao, C.; Tata, B. V. R. *J. Phys.: Condens. Matter* **1991**, *3*, 7973−7982.
(45) van Winkle, D. H.; Murray, C. A. *Phys. Rev. A* **1986**, *34*, 562−573.
(46) Hiltner, P. A.; Papir, Y. S.; Krieger, I. M. *J. Phys. Chem.* **1971**, *75*, 1881−1886.

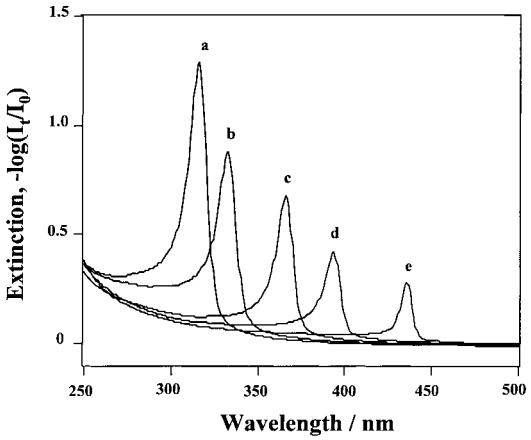

Figure 9. Transmission spectra of PFBMA CCA at different particle concentrations: (a) 10.60%; (b) 7.90%; (c) 6.25%; (d) 5.14%, and (e) 3.60%. Particle diameter was 82 nm. The CCA were 0.50 mm thick.

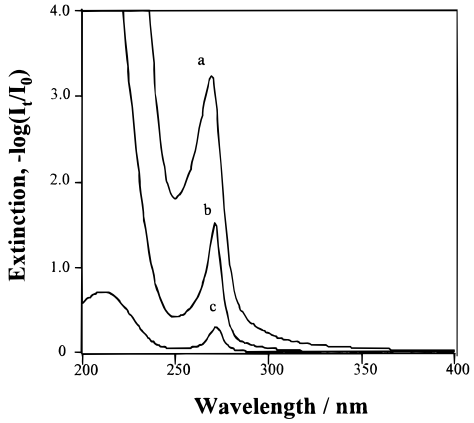

Figure 10. UV optical notch filter made from PFBMA CCA. The particle diameter was 82 nm, and the volume fraction was 17.18%. CCA thickness: (a) 0.80 mm, (b) 0.40 mm, and (c) 0.10 mm. Diffraction occurred at 270 nm. The polymer colloids start to absorb light at 250 nm.

tallites and lattice defects, which broaden the bandwidth.[47] We can see from eq 7 that the bandwidth is proportional to $(m^2 - 1)$. The narrow bandwidths of the fluorinated CCA result from the small refractive index difference between the particles and water.

Near-UV CCA Notch Filter. CCAs can be used as efficient optical notch filters as demonstrated previously by Asher et al.[11,12] Figure 9 shows the transmission spectra of an 82 nm diameter PFBMA CCA at different particle concentrations. The diffraction occurs at 436 nm when the volume fraction is 3.60%. As the concentration of particle increases, the diffraction wavelength decreases to 315 nm for a 10.60% volume fraction because the lattice constant decreases. If the sample is further concentrated to a 17.18% volume fraction, the diffraction peak occurs at 270 nm (Figure 10). This is at the edge of the absorption band of the PFBMA polymer, which begins to significantly absorb light below 250 nm.

Refractive Index Matching CCAs to the Surrounding Medium. We refractive index matched the CCA to the medium by adding methyl phenyl sulfoxide (MPSO), a water-miscible solvent of high refractive index ($n_D = 1.577$), to the CCA. The CCA ordering disappeared after mixing, but returned after shaking with ion-exchange resin for 24 h. Figure 11 shows

(47) Zachariasen, W. H. *Theory of X-ray Diffraction in Crystals*; John Wiley and Sons: New York, 1946; pp 83−155.

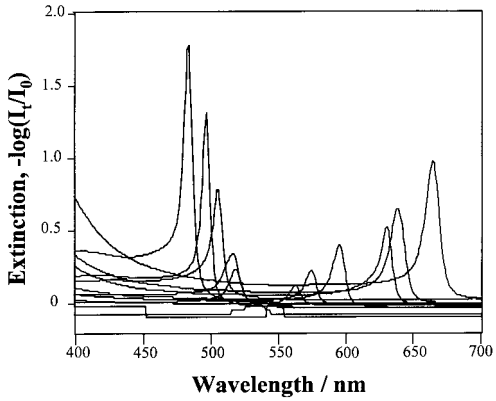

Figure 11. Extinction spectra of liquid PFBMA CCA for different refractive index mismatches between particles and the suspension medium (MPSO/water). From left to right, the refractive indices of the colloid solutions were 1.3390, 1.3500, 1.3605, 1.3667, 1.3757, 1.3853, 1.3972, 1.4080, 1.4152, 1.4253, 1.4362, 1.4467, and 1.4582, respectively. The refractive index of particles was 1.3860 as determined by turbidity measurements (see Figure 5). The particle diameter and volume fraction of the original sample was 116 nm and 10.3%, respectively. The CCA was 0.80 mm thick.

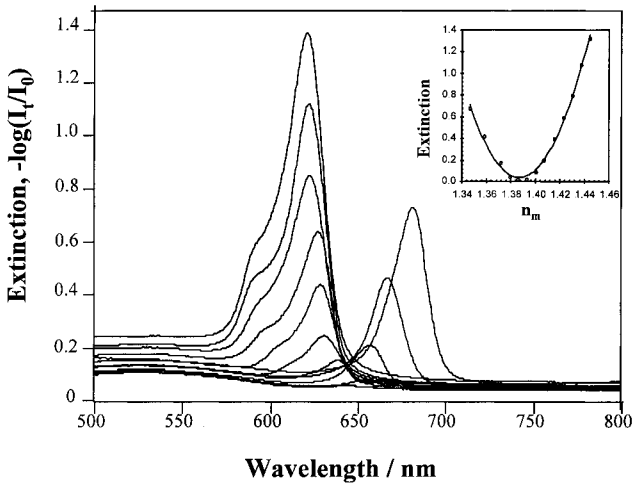

Figure 12. Transmission spectra of PFBMA PCCA in DMSO/water mixtures of different refractive indices. From right to left, the refractive index (n_m) of DMSO/water medium was 1.3330, 1.3458, 1.3600, 1.3685, 1.3750, 1.3830, 1.3907, 1.3980, 1.4070, 1.4150, 1.4226, 1.4304, 1.4375, respectively. The particle diameter was 155 nm. The insert shows that the dependence of the extinction on n_m is quadratic. The refractive index of particles was determined to be 1.3871 at 645 nm.

the transmission spectra from these CCAs at various suspension refractive indexes. The Bragg diffraction wavelength increases with addition of MPSO because of the dilution. No diffraction occurs at the match point, but the diffraction returns after the particles become over-index matched. Thus, transparent aqueous CCAs can be prepared from these highly fluorinated particles.

It is more convenient to refractive index match the particles to the medium in a hydrogel polymerized CCA (PCCA) compared to the aqueous CCA because the CCA ordering is locked permanently by the hydrogel network. We refractive index matched a PCCA by adding DMSO to the aqueous medium (Figure 12). The diffraction wavelength decreases as DMSO is added because the gel shrinks upon DMSO addition. The diffraction extinction initially decreases, disappears, and then increases again as n_m increases. According to the diffraction theory,[46] extinction should be proportional to $(m^2 - 1)$, as

is experimentally observed in the parabolic relationship with m as seen in the insert of Figure 12.

Summary

We synthesized highly charged, low refractive index (n_D = 1.3860), monodisperse dyed poly(1H,1H-heptafluorobutyl methacrylate) colloidal spheres by emulsion polymerization. After dialysis and ion exchange, these particles formed well-ordered CCAs, which Bragg diffract light in a wide spectral range, with narrow bandwidths due to the small refractive index difference between the particles and the aqueous medium. We permanently locked the CCA ordering within a polyacrylamide hydrogel matrix and refractive index matched the CCA to the gel medium. The refractive index matched polymerized dyed CCA can be used in nanosecond fast optical switching and limiting devices as discussed in the accompanying paper.

Acknowledgment. We thank S.-Y. Chang, Z. Wu, J. Holtz, L. Liu, H. B. Sunkara, and J. M. Weissman for helpful discussions. This work was supported by the Office of Naval Research through Grant No. N00014-94-0592 and by the National Science Foundation (CHE 9633561).

Appendix

Colloidal particles prepared from $Na_2S_2O_8$-initiated emulsion polymerization consist of many entangled polymer chains: $^{-}SO_4-(CH_2-CHR)_n^{-}$. The sulfate ($SO_4^{-}$) endgroups are hydrophilic and migrate to the surface of the particles. Each chain will contribute one charge to the particle. If each particle has Z polymer chains, the number of particle surface charge will be Ze^{-}. Thus the average number polymer molecular weight (M_n) can be calculated as

$$M_n = \frac{\text{particle molecular weight}}{\text{no. of polymer chains per particle}} = N_A(^1/_6)\pi(d \times 10^{-7})^3\rho/Z \quad (9)$$

where N_A is Avogadro constant, d is the particle diameter (nm), and ρ is polymer density (g/cm^3). If the particle surface charge density is expressed as σ (μC/cm^2), then

$$\sigma = Z(1.608 \times 10^{-19})10^6/(\pi\,(d \times 10^{-7})^2) \quad (10)$$

Combining eqs 9 and 10, we have

$$\sigma = (1.61 \times 10^3)d\rho/M_n \quad (11)$$

Thus, the particle surface charge density is inversely proportional to the polymer molecular weight.

JA9804823